Altered gut microbe metabolites in patients with alcohol-induced osteonecrosis of the femoral head: An integrated omics analysis

CHEN YUE[1*], MAOXIAO MA[2*], JIAYI GUO[2], HONGJUN LI[2], YUXIA YANG[2], YOUWEN LIU[2] and BIN XU[3]

[1]Evidence Based Medicine Center and [2]Department of Orthopedics, Luoyang Orthopedic-Traumatological Hospital of Henan Province, Luoyang, Henan 471002; [3]Department of Orthopedics, Tongde Hospital of Zhejiang Province, Hangzhou, Zhejiang 310012, P.R. China

Received July 18, 2023; Accepted March 19, 2024

DOI: 10.3892/etm.2024.12599

Abstract. Excessive alcohol consumption is considered to be a major risk factor of alcohol-induced osteonecrosis of the femoral head (AONFH). The gut microbiota (GM) has been reported to aid in the regulation of human physiology and its composition can be altered by alcohol consumption. The aim of the present study was to improve the understanding of the GM and its metabolites in patients with AONFH. Metabolomic sequencing and 16S rDNA analysis of fecal samples were performed using liquid chromatography-mass spectrometry to characterize the GM of patients with AONFH and healthy normal controls (NCs). Metagenomic sequencing of fecal samples was performed to identify whether GM changes on the species level were associated with the expression of gut bacteria genes or their associated functions in patients with AONFH. The abundance of 58 genera was found to differ between the NC group and the AONFH group. Specifically, *Klebsiella*, *Holdemanella*, *Citrobacter* and *Lentilactobacillus* were significantly more abundant in the AONFH group compared with those in the NC group. Metagenomic sequencing demonstrated that the majority of the bacterial species that exhibited significantly different abundance in patients with AONFH belonged to the genus *Pseudomonas*. Fecal metabolomic analysis demonstrated that several metabolites were present at significantly different concentrations in the AONFH group compared with those in the NC group. These metabolites were products of vitamin B6 metabolism, retinol metabolism, pentose and glucuronate interconversions and glycerophospholipid metabolism. In addition, these changes in metabolite levels were observed to be associated with the altered abundance of specific bacterial species, such as *Basidiobolus*, *Mortierella, Phanerochaete* and *Ceratobasidium*. According to the results of the present study, a comprehensive landscape of the GM and metabolites in patients with AONFH was revealed, suggesting the existence of interplay between the gut microbiome and metabolome in AONFH pathogenesis.

Correspondence to: Dr Bin Xu, Department of Orthopedics, Tongde Hospital of Zhejiang Province, 234 Gu-cui Road, Hangzhou, Zhejiang 310012, P.R. China
E-mail: spotxu@163.com

Dr Youwen Liu, Department of Orthopedics, Luoyang Orthopedic-Traumatological Hospital of Henan Province, 82 South Qiming Road, Luoyang, Henan 471002, P.R. China
E-mail: liuyouwen543@sina.com

*Contributed equally

Key words: gut microbiota, metagenomics, metabolite, osteonecrosis of the femoral head, alcohol

Introduction

Osteonecrosis of the femoral head (ONFH) is a common orthopedic disease caused by a decrease in blood supply to the femoral head, with frequently reported features of osteocyte necrosis, trabecular bone fracture and articular surface collapse (1). It is estimated that there are ~8.12 million individuals over the age of 15 years with ONFH in China and the total number of patients with ONFH worldwide will reach 20 million in the next 10 years (2). ONFH can be categorized into traumatic ONFH and non-traumatic ONFH, with the latter being further categorized into steroid- or corticosteroid-induced ONFH (SONFH) and alcohol-induced ONFH (AONFH) (3). Excessive alcohol consumption is recognized to be a major risk factor for AONFH (4). Aberrant alcohol metabolism may contribute to femoral head tissue damage through the production of a number of toxic byproducts, such as acetaldehyde, free radicals and acetaldehyde adducts. In addition, alcohol metabolic impairments can adversely affect intravascular coagulation and the clotting cascade (4,5). However, the pathogenic mechanism of AONFH remains poorly understood.

The gut microbiota (GM) has been reported to be an important symbiotic partner in the regulation of human physiology (6). A number of studies have previously reported that gut microbiome composition and corresponding metabolic activity can participate in the regulation of bone homeostasis to exert pivotal effects on the development of osteochondral or bone diseases (6,7). These include estrogen deprivation-induced bone loss (8) and bisphosphonate-related osteonecrosis of the jaw (9). In addition, alcohol consumption can alter the GM composition and is related to overall health, and cause diseases such as inflammatory bowel disease, gastrointestinal cancers

and liver injury (10). However, to the best of our knowledge, the interaction among alcohol, the GM and GM metabolites, in addition to their roles in the development of ONFH, has not been reported to date.

On the basis of the previously reported regulatory effects of GM on bone (6,7), it may be hypothesized that alcohol-induced gut dysbiosis may participate in the development of AONFH. Therefore, in the present study, fecal integrated omics analysis was performed, including 16S rDNA gene sequencing, metagenomic and metabolomic analyses, to define the gut metabolome and metabolic profiles in patients with AONFH.

Materials and methods

Sample collection and ethical approval. The present study enrolled 98 Chinese men, including 48 healthy adults [negative control (NC); age, 41.75±10.50 years] and 50 patients with AONFH (age, 43.98±11.40 years), from June 2021 to June 2022 at the Luoyang Orthopedic-Traumatological Hospital of Henan Province (Luoyang, China). The selected participants were Han Chinese from similar geographic areas, experienced the same environmental factors, with similar hygiene status and diet (except alcohol consumption).

The patients with AONFH were required to meet the following inclusion criteria: i) Aged 18-80 years; ii) history of any type of alcoholic beverage intake of >320 ml/week for >6 months (11); iii) AONFH diagnosis within 1 year of alcohol consumption at the aforementioned levels; iv) AONFH diagnosed by clinical examination, X-ray, CT and MRI; and v) no history of other osteoarticular diseases (such as injury, osteoarthritis, rheumatoid arthritis, gout or skeletal fluorosis), chronic diseases (hypertension, diabetes or coronary heart disease) or bowel diseases (inflammatory bowel disease, irritable bowel syndrome or colorectal cancer), for which they received treatment in the past 6 months. The exclusion criteria of healthy controls were as follows: i) Musculoskeletal pathologies or recent injuries; and ii) use of antibiotics, probiotics, prebiotics or symbiotics in the previous 2 months.

The general clinical data of patients were recorded, including age, educational background, height, weight and BMI. The present study was approved by the ethics committee of Luoyang Orthopedic-Traumatological Hospital of Henan Province (approval no. KY2021-007-01). All participants provided written informed consent for participation into the present study and the study protocols followed the ethical guidelines of The Declaration of Helsinki. Fecal samples were collected by the participants and immediately transported to the laboratory, where they were divided into three portions per sample, packed into three freezer tubes, frozen in liquid nitrogen overnight and preserved at -80˚C for further testing.

DNA extraction and 16S rDNA gene sequencing. A total of 48 NC samples and 50 AONFH samples were subjected to 16S rDNA gene sequencing analysis. DNA was extracted using the E.Z.N.A.® Stool DNA Kit (cat. no. D4015; Omega Bio-Tek, Inc.) according to the manufacturer's protocols. Nuclease-free water was used as the negative control. Total DNA from each sample was eluted in 50 μl elution buffer and stored at -80˚C until PCR was performed.

The V3-V4 region of the prokaryotic 16S rDNA gene was amplified using the following primers: 341 forward, 5'-CCT ACGGGNGGCWGCAG-3'; and 805 reverse, 5'-GACTAC HVGGGTATCTAATCC-3' (N, A+C+G+T; H, A+C+T; V, A+C+G; W, A+T) (12). The 5' ends of the primers were tagged with specific barcodes for each sample, which were sequenced using universal primers (forward, 5'-GTGCCAGCMGCCGCG GTAA-3'; reverse, 5'-GGACTACHVGGGTWTCTAAT-3'). PCR amplification was performed in a reaction mixture with a total volume of 25 μl, containing 25 ng template DNA, 12.5 μl PCR premix, 2.5 μl of each primer and PCR-grade water to adjust to the final volume, 1 μl of KOD DNA polymerase (2.5 U/μl; Toyobo). The PCR conditions used to amplify the prokaryotic 16S fragments were as follows: Initial denaturation at 98˚C for 30 sec; followed by 32 cycles of 98˚C for 10 sec, 54˚C for 30 sec and 72˚C for 45 sec and a final extension at 72˚C for 10 min. PCR product amplification was confirmed using 2% agarose gel electrophoresis (Genecolour™; GBY-II; Beijing Jinboyi Biotechnology Co., Ltd). Throughout the DNA extraction process, ultrapure water was used instead of sample solution as a negative control to exclude the possibility of false-positive PCR results. The PCR products were purified using AMPure XT beads (Beckman Coulter, Inc.) and quantified using Qubit 3.0 fluorometer (Invitrogen; Thermo Fisher Scientific, Inc.). The final library DNA concentration was 10 ng/μl. The amplicon pools were prepared for sequencing and the size and quantity of the amplicon library were assessed using an Agilent 2100 Bioanalyzer (Agilent Technologies, Inc.) and the Library Quantification Kit for Illumina (Kapa Biosystems; Roche Diagnostics), respectively. The libraries were sequenced using the NovaSeq PE250 platform according to the manufacturer's instructions (Illumina, Inc.).

The raw 150 bp paired-end reads were assigned to samples based on their unique barcodes and truncated by cutting off the barcode and primer sequence. Paired-end reads were merged using FLASH (version 1.2.8; http://ccb.jhu.edu/software/FLASH/). Quality filtering of the raw reads was performed to obtain high-quality clean tags using 'fqtrim' (version 0.94, http://ccb.jhu.edu/software/fqtrim/). Chimeric sequences were filtered using Vsearch software (version 2.3.4; https://github.com/torognes/vsearch). Dereplication with DADA2 (13) generated a feature table and feature sequence. Alpha diversity and beta diversity were calculated using QIIME2 (version 2019.7; https://qiime2.org/), for which the same number of sequences were extracted randomly by reducing the number of sequences to the minimum for certain samples, and the relative abundance was used to determine the bacterial taxonomy. Alpha diversity and beta diversity figures were produced using the ggplot2 (version 3.2.0) toolbox implemented in R software. Blast (http://www.ncbi.nlm.nih.gov/BLAST) was used for sequence alignment and each representative feature sequence was annotated using the SILVA database (version 138.1, http://www.arb-silva.de) (14).

Fecal metagenomics analysis. As one sample from the NC group was missed in the *fecal metagenomics analysis*, a total of 47 NC and 50 AONFH fecal samples were subjected to metagenomics analysis. The DNA library was constructed using a TruSeq Nano DNA LT Library Preparation Kit (cat. no. FC-121-4001; Illumina, Inc.). DNA was fragmented

using dsDNA Fragmentase (cat. no. M0348S; New England BioLabs, Inc.) and incubated at 37˚C for 30 min, before the sequencing library was constructed from the fragmented cDNA. Blunt-end DNA fragments were generated using a combination of fill-in reactions and exonuclease activity, and size selection was performed with the provided sample purification beads. An A-base was then added to the blunt ends of each strand, preparing them for ligation to the indexed adapters. Each adapter contained a T-base overhang for ligating the adapter to the A-tailed fragmented DNA. These adapters contained the full complement of sequencing primer hybridization sites for single, paired-end and indexed reads. Single- or dual-index adapters were ligated to the fragments and the ligated products were amplified by PCR using the following thermocycling conditions: Initial denaturation at 95˚C for 3 min; followed by 8 cycles of 98˚C for 15 sec, 60˚C for 15 sec and 72˚C for 30 sec and a final extension at 72˚C for 5 min.

Raw sequencing reads were processed to obtain valid reads for further analysis. First, sequencing adapters were removed from sequencing reads using 'cutadapt' (version 1.9, http://cutadapt.readthedocs.org/en/stable/guide.html). The low-quality reads were then trimmed by 'fqtrim' (version 0.94, http://ccb.jhu.edu/software/fqtrim/) using a sliding-window algorithm. The reads were next aligned to the host genome using 'bowtie2' (version 2.2.0) to remove host DNA contamination (15). Once quality-filtered reads were obtained, they were *de novo* assembled to construct the metagenome for each sample using IDBA-UD (version 1.1.1) (16). All coding regions (CDS) within the metagenomic contigs were predicted using 'MetaGeneMark' (version 3.26) (17). CDS sequences from all samples were clustered using CD-HIT (version 4.6.1) to obtain unigenes (18). Unigene abundance for individual samples were estimated by transcripts per million based on the number of aligned reads using bowtie2 (version 2.2.0). The lowest common taxonomic ancestors of the unigenes were obtained by aligning them against the National Center for Biotechnology Information Non-Redundant Protein Sequence database using DIAMOND (version 0.9.14) (19). Similarly, the functional annotation of unigenes were obtained using Gene Ontology (GO) database (version go_2018.12.21, http://www.geneontology.org/) Kyoto Encyclopedia of Genes and Genomes (KEGG-release_87.1, http://www.genome.jp/kegg/).

A random forest model was constructed using the random forest package in R software (version 3.4.4). Receiver operating characteristic (ROC) curves were generated and the area under the curve (AUC) values were computed using pROC in R software. Functional annotation of the unigenes was also performed using Blast (http://www.ncbi.nlm.nih.gov/BLAST). Finally, differentially expressed unigenes were identified at the taxonomic, functional or gene level by Fisher's exact test based on the taxonomic annotation, functional annotation and abundance profiles, respectively.

Metabolomics and data analysis. One sample from the AONFH group was missed in the metabolomics analysis, so a total of 48 NC samples and 49 AONFH samples were subjected to metabolomics analysis. The metabolites were extracted from fecal samples with 50% methanol buffer and incubated at 24˚C for 10 min. The extraction mixture was stored overnight at -20˚C. After centrifugation at 4,000 x g for 20 min at room temperature, the supernatants were transferred into 96-well plates and stored at -80˚C prior to being subjected to liquid chromatography-mass spectrometry (LC-MS) analysis to identify the metabolites. Pooled quality control (QC) samples were prepared by combining 10 μl each extraction mixture. Chromatographic separation was performed using the UltiMate 3000 high-performance LC system (Thermo Fisher Scientific, Inc.). No internal standard was used (20). An ACQUITY UPLC BEH C18 column (size, 100x2.1 mm; 1.8 μm; Waters Corporation) was used for the reversed phase separation. The column temperature was maintained at 35˚C. The flow rate was 0.4 ml/min, and the mobile phase consisted of solvent A (water, 0.1% formic acid) and solvent B (acetonitrile, 0.1% formic acid). The gradient elution conditions were as follows: 0-0.5 min, 5% solvent B; 0.5-7 min, 5-100% solvent B; 7-8 min, 100% solvent B; 8-8.1 min, 100-5% solvent B; 8.1-10 min, 5% solvent B. The injection volume for each sample was 4 μl.

A high-resolution triple time-of-flight (TOF) 5600 Plus tandem mass spectrometer (SCIEX) was operated in both positive ionization mode and negative ionization mode for detecting metabolites eluted from the column. The curtain gas was set to 30 psi, ion source gas1 was set to 60 psi, ion source gas2 was set to 60 psi and the interface heater temperature was set to 650˚C. For positive ion mode, the Ionspray voltage was set at 5,000 V. For negative ion mode, the Ionspray voltage was set at -4,500 V. The mass spectrometry data were acquired in information-dependent acquisition mode. The TOF mass range was in the 60-1,200-Da range. The survey scans were acquired in 150 msec, and ≥12 product ion scans were collected if they reached the threshold of >100 counts/sec with a 1+ charge-state. The total cycle time was fixed at 0.56 sec. A total of four-time bins were summed for each scan at a pulser frequency value of 11 kHz through monitoring the 40 GHz multichannel thermal conductivity detector with four-anode/channel detection. Dynamic exclusion was set at 4 sec. During acquisition, the mass accuracy was calibrated every 20 samples. Furthermore, to evaluate the stability of the LC-MS procedure throughout acquisition, a QC sample (pooled sample) was processed after every 10 samples. The following multiple reaction monitoring transitions were selected: m/z 1861.3→70.02 (positive), m/z 1889.0→72.02 (negative).

The acquired MS data were pretreated by peak picking, peak grouping, retention time correction, second peak grouping and annotation of isotopes and adducts using the XCMS software. LC-MS raw data files were converted into the 'mzXML' format and then processed using XCMS, CAMERA and the metaX toolbox implemented with the R software (version 3.5.3 R Core Team, 2019; https://www.R-project.org/). Each ion was identified by combining the retention time and m/z data. The intensity of each peak was recorded and a 3D matrix containing arbitrarily assigned peak indices (retention time-m/z pairs), sample names (observations) and ion intensity information (variables) was generated.

The KEGG and Human Metabolome Database (HMDB 5.0, http://www.hmdb.ca) databases were used to annotate the metabolites by matching the exact molecular mass data (m/z) of samples with those from the databases. If the mass difference between the observed and database values was <10

Table I. Characteristics of participants in the present study.

Characteristic[a]	Patients with alcohol-induced osteonecrosis of the femoral head (n=50)	Negative controls (n=48)	P-value
Age, years	43.98±11.40	41.75±10.50	0.32
Height, cm	172.64±5.30	174.58±5.76	0.09
Weight, kg	72.46±11.74	71.19±11.48	0.59
BMI, kg/m^2	24.31±3.79	23.35±3.54	0.20
Alcohol consumption	50 (100)	0 (0)	<0.001
Smoking	4 (8)	0 (0)	0.12

[a]Data are presented as either the mean ± standard deviation or n (%).

parts per million, the metabolite would be annotated, and the molecular formula of the metabolite would be further identified and validated by isotopic distribution measurements. An in-house metabolite fragment spectrum library was used to validate the identified metabolites (21).

Peak intensity data were further preprocessed using metaX. Features that were detected in <50% of QC samples or 80% of biological samples were removed and the remaining peaks with missing values were imputed using the 'k-nearest neighbor' algorithm to further improve data quality (22). Principal component (PC) analysis was performed for outlier detection and batch effect evaluation using the pre-processed dataset. QC-based robust locally weighted scatter-plot smoother signal correction was then fitted to the QC data with respect to the order of injection to minimize signal intensity drift over time. In addition, the relative standard deviations of the metabolic features were calculated across all QC samples and any that were >30% were removed.

Unparied Student's t-tests were conducted to detect differences in metabolite concentrations between the two groups. The P-value was adjusted for multiple tests with a false-discovery rate (FDR) using the Benjamini-Hochberg method. A median FDR<0.05 was used as a cutoff value. Supervised partial least squares discriminant analysis (PLS-DA) was conducted using metaX to discriminate between the different variables whereas the XCMS software was used to pretreat the acquired MS data. The raw LC-MS raw data files were processed with metaX using the 'XCMS' package for peak detection and the 'CAMERA' package for peak annotation in R. The variable importance in projection (VIP) was calculated, where a VIP cut-off value of 1.0 was used to select important features.

Statistical analysis. Continuous variables were presented as the mean ± standard deviation (SD) and Student's t-test or the Wilcoxon signed-rank test was used to compare their differences. Pearson's chi-squared test or Fisher's exact test was used to compare differences for count data. Spearman's correlation analysis was conducted to calculate the correlation between species and metabolites. P<0.05 was considered to indicate a statistically significant difference. All data were analyzed using GraphPad Prism software (version 6; Dotmatics), R software and Microsoft Excel (version 3.3.2.13, Microsoft Corp.).

Results

Characteristics of the study population. A total of 50 patients with AONFH and 48 healthy adults were included in the present study. The demographic characteristics of the two groups did not show any statistically significant difference (Table I), suggesting that there were no confounding factors that could have influenced the results.

GM changes in patients with AONFH. To identify changes in the gut microbiome in patients with AONFH, 16S rRNA metagenomics analysis was conducted on 98 fecal samples, including 48 samples from the NC group and 50 samples from the AONFH group. After QC, >21 million valid bases were obtained for each sample (Table SI).

The rRNA sequences were then grouped into operational taxonomic units (OTUs) based on sequence similarity to classify the microbial diversity in terms of bacterial strains. Performing a 97% similarity cluster analysis identified 4,966 OTUs in the NC group and 4,248 OTUs in the AONFH group, where 1,697 OTUs were shared between the two groups (Fig. 1A).

Alpha diversity analysis was then used to analyze the complexity of species diversity in each sample using several indices, including the observed OTUs, Chao1, Shannon and Simpson indices. The richness and diversity rarefaction curve in the two groups tended to be flat or reach a plateau, suggesting satisfactory sequencing depth (Fig. S1). Alpha diversity analysis demonstrated no significant differences in observed OTUs, Chao1, Shannon and Simpson indices between the NC group and the AONFH group (Fig. S2), which indicated that the complexity of species diversity was similar.

Principle coordinate analysis (PCoA) and analysis of similarities (ANOSIM) testing for beta diversity demonstrated a significant difference in GM composition and abundance between the two groups (unweighted Unifrac P=0.005 and Jaccard P=0.003; Fig. 1B and C).

AONFH-related changes in gut microbiome composition. Taxon-dependent analysis (Fig. 1D) identified 31 phyla present in both groups, with Firmicutes, Actinobacteriota, Proteobacteria, Bacteroidota and Verrucomicrobiota being the most dominant phyla. Firmicutes was the most predominant

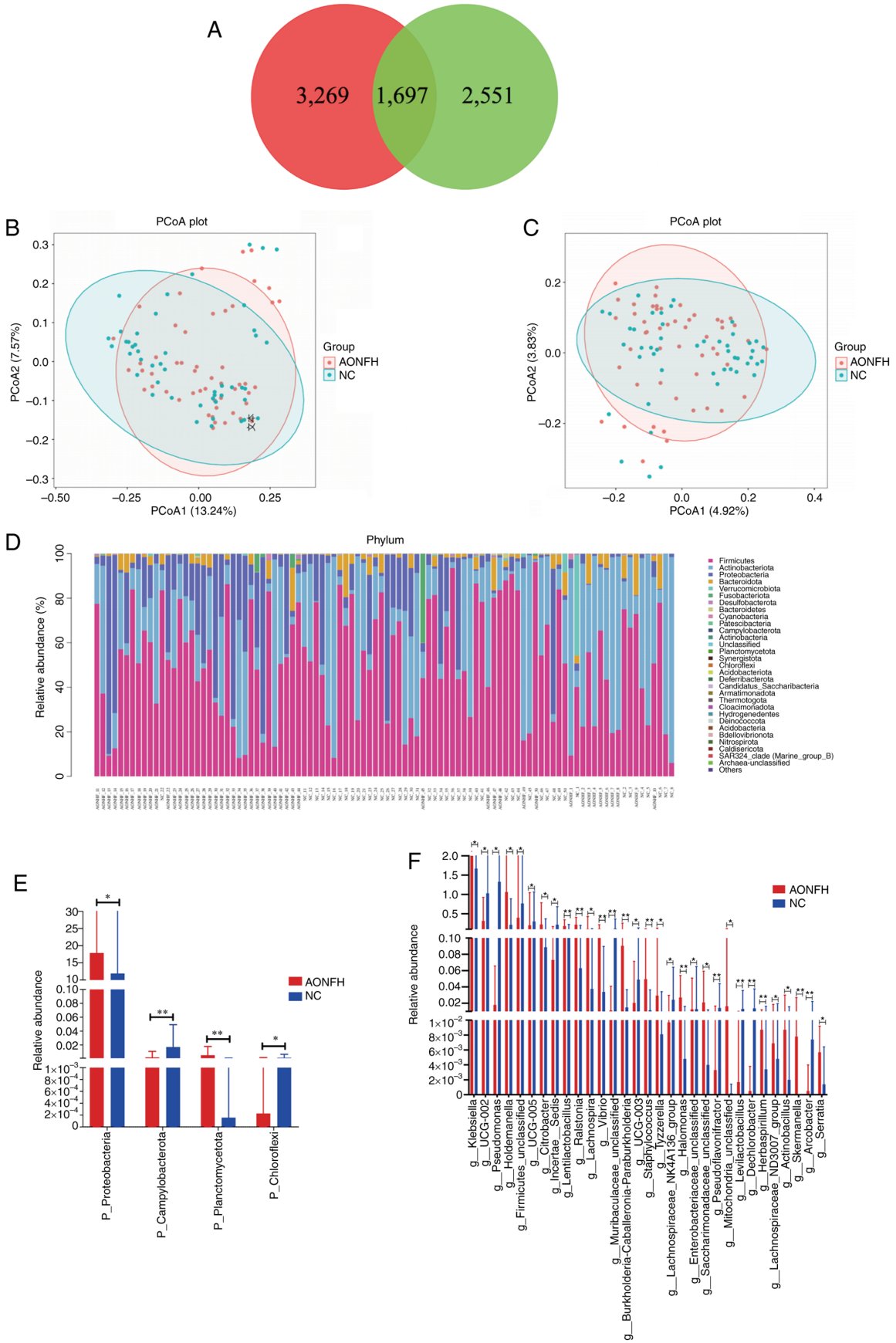

Figure 1. Gut microbiome diversity and structure analysis of patients with AONFH and NCs. (A) Venn diagram of the observed features (amplicon sequence variants) in the AONFH and NC groups. PCoA of the microbiota based on (B) unweighted UniFrac (ANOSIM, R=0.058, P=0.005) and (C) Jaccard (ANOSIM, R=-0.060, P=0.003) distance matrices for the AONFH and NC groups. (D) Heatmap was generated at phylum level based on the relative abundance values. Statistically significant differences in bacterial abundance at the (E) phylum and (F) genus level between the AONFH and NC groups (mean ± SD). *P<0.05, **P<0.01. AONFH, alcohol-induced osteonecrosis of the femoral head; NC, negative control; PCoA, principal coordinate analysis; ANOSIM, analysis of similarities; p_, at phylum level, g_, at genus level.

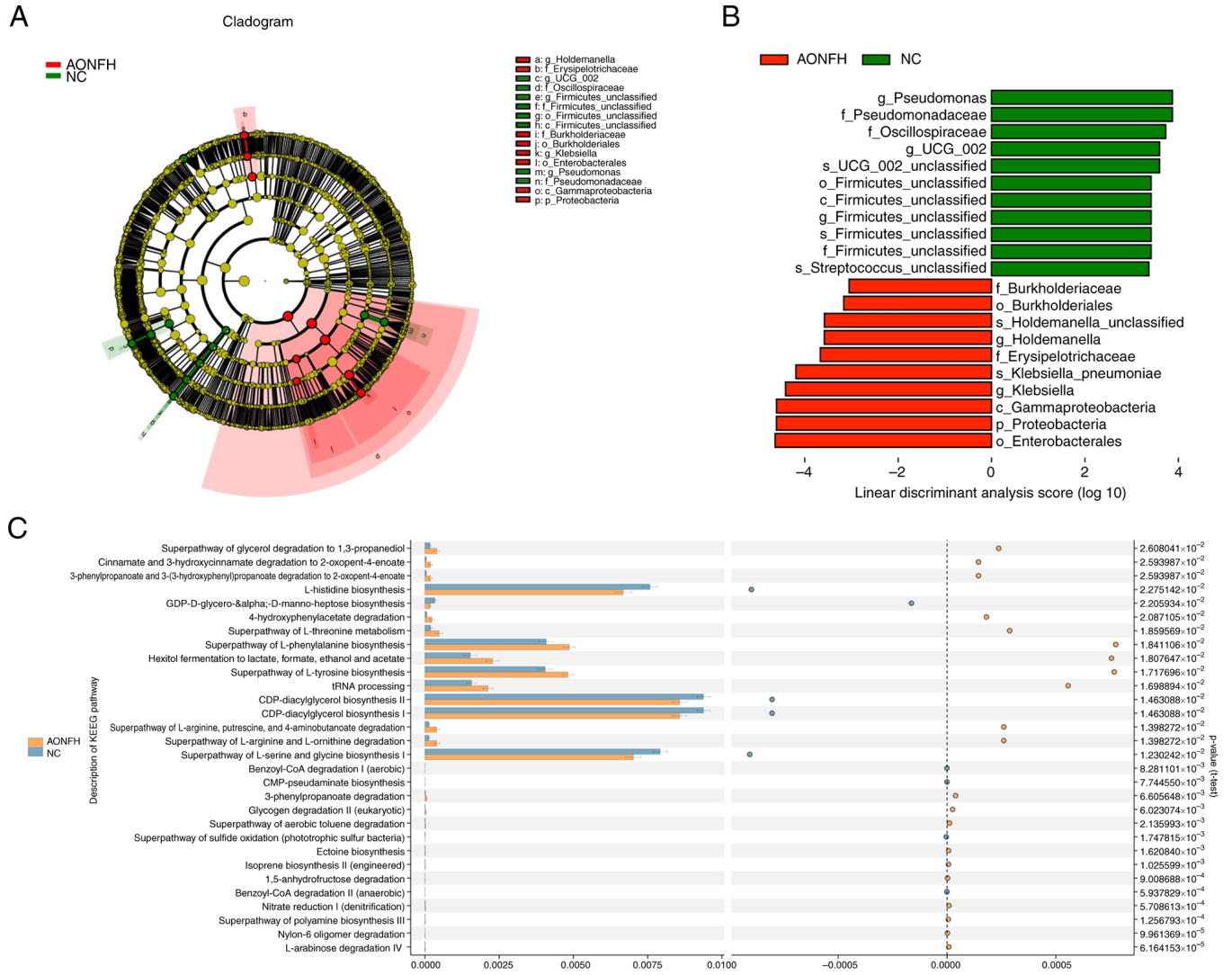

Figure 2. Gut microbiome composition and functional analyses. (A) Cladogram indicating the phylogenetic distribution of the microbiota in the AONFH and NC groups. (B) Linear discriminant analysis integrated with effect size demonstrated differences in abundance between the AONFH and NC groups. (C) Predicted functions of the gut microbiota based on KEGG pathway analysis. The extended error bar plot demonstrated the significantly different KEGG pathways between the AONFH and NC groups. AONFH, alcohol-induced osteonecrosis of the femoral head; NC, negative control; KEGG, Kyoto Encyclopedia of Genes and Genomes. p, phylum; c, class; o, order; f, family; g, genus; s, species.

phylum, accounting for 55.23 and 48.19% of the GM in the NC group and the AONFH group, respectively. Further analyses demonstrated that, at the phylum level, Campylobacterota (P=0.0048) and Chloroflexi (P=0.0392) were significantly more abundant in the NC group compared with those in the AONFH group, whereas Planctomycetota (P=0.0099) and Proteobacteria (P=0.0438) were significantly more abundant in the AONFH group compared with those in the NC group (Fig. 1E).

At the genus level, the abundance of 58 genera was significantly different between the NC group and the AONFH group. Among them, *UCG-002* (P=0.0241), *Pseudomonas* (P=0.0342), *UCG-005* (P=0.0436) and *Incertae sedis* (P=0.0208) were significantly more abundant in the NC group compared with those in the AONFH group, whereas *Klebsiella* (P=0.0232), *Holdemanella* (P=0.0229), *Citrobacter* (P=0.0468) and *Lentilactobacillus* (P=0.0093) were significantly more abundant in the AONFH group compared with the NC group (Fig. 1F).

Next, linear discriminant analysis (LDA) was performed and integrated with effect size to generate a cladogram to identify the specific bacteria species that dominate in the GM of patients with AONFH (Fig. 2A). Significant differences were demonstrated in 21 OTUs (LDA>3), including *Pseudomonas*, Pseudomonadaceae, Oscillospiraceae, *UCG-002*, Firmicutes and *Streptococcus*, which were more abundant in the NC group compared with those in the AONFH group. By contrast, Burkholderiaceae, Buekholderiales, *Holdemanella*, Erysipelotrichaceae, *Klebsiella pneumoniae*, *Klebsiella*, Gammaproteobacteria, Proteobacteria and Enterobacterales were more abundant in the AONFH group compared with those in the NC group (Fig. 2B).

Prediction of gene function in the GM. Next, Phylogenetic Investigation of Communities by Reconstruction of Unobserved States (PICRUSt 2.2.0b http://huttenhower.sph.harvard.edu/galaxy/root?tool_id=PICRUSt_normalize) was used to compare gut microbial gene functions across Clusters

of Orthologous Genes (COGs), KEGG and KEGG orthology functional orthologues between the AONFH and NC groups (Figs. S3-5). KEGG pathway analysis identified important functions, such as 'CDP-diacylglycerol biosynthesis I/II', 'L-histidine biosynthesis' and 'superpathway of L-serine and glycine biosynthesis I' (Fig. 2C), whereas COG database analysis highlighted 'Flp pilus assembly protein TadG', 'lipid-binding SYLF domain' and 'CBS-domain-containing membrane proteins' in the AONFH group were higher when compared with the NC group (Fig. S3). KEGG analysis indicated that gut microbial genes were upregulated in AONFH group, such as those participating in 'propanoate metabolism', 'fructose and mannose metabolism' and 'phosphotransferase system'. However, those participating in RNA degradation and transcription machinery were downregulated (Fig. S4). KEGG orthology analysis indicated that 'AgrD protein', 'formate dehydrogenase', 'diapolycopene oxygenase', 'kumamolisin' and 'carotenoid cleavage dioxygenase' were enhanced in the AONFH group (Fig. S5).

Metagenomic sequencing demonstrates significant differences between the AONFH and NC groups. Metagenomic sequencing was performed on fecal samples from 50 patients with AONFH and 47 healthy individuals. A total of 317,243 genes were identified. The samples from the NC group contained 3,177 specific genes that were not detected in the AONFH samples. Compared with the NC group, 20,823 unigenes were found to be differentially expressed in the AONFH group (10,171 upregulated and 10,652 downregulated).

The alpha diversity was lower in the AONFH group compared with that in the NC group, as measured by the observed species and Chao1 indices, Whilst the Shannon and Simpson indices did not demonstrate any significant difference in alpha diversity between the groups (Fig. S6). The results indicated that the complexities of species diversity of the two groups were similar, although the species richness was lower in the AONFH group.

PCoA and ANOSIM testing for beta diversity demonstrated no significant difference in microbial composition between the AONFH and NC groups at the species level (Bray-Curtis Unifrac P=0.06; Fig. 3A). Comparing the profiles of the AONFH and NC groups demonstrated that *Pseudomonas*, *Pseudomonas fluorescens*, *Pseudomonas sp*. TMW-2.1634, *Pseudomonas weihenstephanensis* and *Pseudomonas fragi* were significantly less abundant in the AONFH group compared with those in the NC group (Fig. 3B and Table SII).

Potential role of GM biomarkers in AONFH risk assessment. A random forest model was constructed based on the genera that demonstrated significantly different abundances to identify potential diagnostic biomarkers that could be used to predict AONFH. The optimal model that provided the best discriminatory power utilized 20 genera (Fig. 3C). According to the aforementioned analysis, there were significant differences in the composition of the microbial community between AONFH and NC groups. Therefore, to determine the ability of the identified bacterial biomarkers to discriminate between the two groups, receiver operating characteristic curves were produced and the AUC was calculated. The top five AUC values were for *Enhygromyxa salina* (89.47%), *Hyphomonas beringensis* (87.84%), *Thermococcus profundus* (87.41%), *Syncephalastrum racemosum* (86.93%) and *Roseovarius nitratireducens* (86.91%; Fig. 3D).

Functional analysis of differentially expressed genes in the AONFH group identified by metagenomic sequencing. The top 10 GO items for the three types of gene classifications provided by the GO database were selected (Fig. S7A). Next, GO enrichment analysis of the differentially expressed unigenes between the two groups was performed and the top 20 GO terms were analyzed (Fig. S7B). KEGG analysis of the differentially expressed unigenes was then performed to identify the metabolic pathways that differed most significantly between the two groups. The expression of genes related to 'starch and sucrose metabolism', 'RNA degradation', 'pentose and glucuronate interconversions', 'glutathione metabolism', 'flagellar assembly' and 'bacterial chemotaxis' differed significantly between the AONFH and NC groups ($P \leq 0.01$; unigene number >50; Fig. S7C and Table SIII).

Metabolomic analysis reveals abnormal metabolic alterations in patients with AONFH. To identify changes in the gut microbiome in patients with AONFH, metabolomic analysis was performed on 97 fecal samples, including 48 samples from the NC group and 49 samples from the AONFH group. PLS-DA was performed to identify discriminant metabolites in the fecal samples from these two groups. Using negative ion mode (NIM), there was an apparent trend towards the separation of metabolic features in the fecal samples from patients with AONFH and NCs (Fig. 4A). The combined explained variance of PC1 and PC2 (Fig. 4B) was 18.84%, R^2=(PC1, 0.0; PC2, 0.6568) and Q^2=(PC1, 0.0; PC2, -0.3303). In positive ion mode (PIM), there was also an apparent trend toward separation between the metabolic features of the fecal samples from patients with AONFH and NCs (Fig. 4C). The combined explained variance of PC1 and PC2 was 18.41% (Fig. 4D), R^2=(PC1, 0.0; PC2, 0.6386) and Q^2=(PC1, 0.0; PC2 -0.3213).

Fecal metabolomic changes in patients with AONFH. Metabolomic analysis identified 21,486 features and 11,723 metabolites in PIM and 14,155 and 7,576 metabolites in NIM. The obtained data were used as the batch query against the HMDB for single-stage mass spectrometry analysis, which annotated 5,098 and 3,689 individual samples with the features identified in PIM and NIM, respectively. In the HMDB superclass analysis, the most abundant metabolites were 'lipids and lipid-like molecules' and 'organic acid and derivatives' (Fig. 5A).

Comparative metabolomic analysis demonstrated clear differences in fecal metabolite profiles between patients with AONFH and NCs (Fig. 5B). A total of 483 significantly upregulated and 396 significantly downregulated metabolites in PIM, whereas 358 significantly upregulated and 296 significantly downregulated metabolites in NIM were identified, in the AONFH group compared with those the control group (Table SIV). These metabolites can potentially be regarded as part of various signaling pathway networks underlying AONFH occurrence.

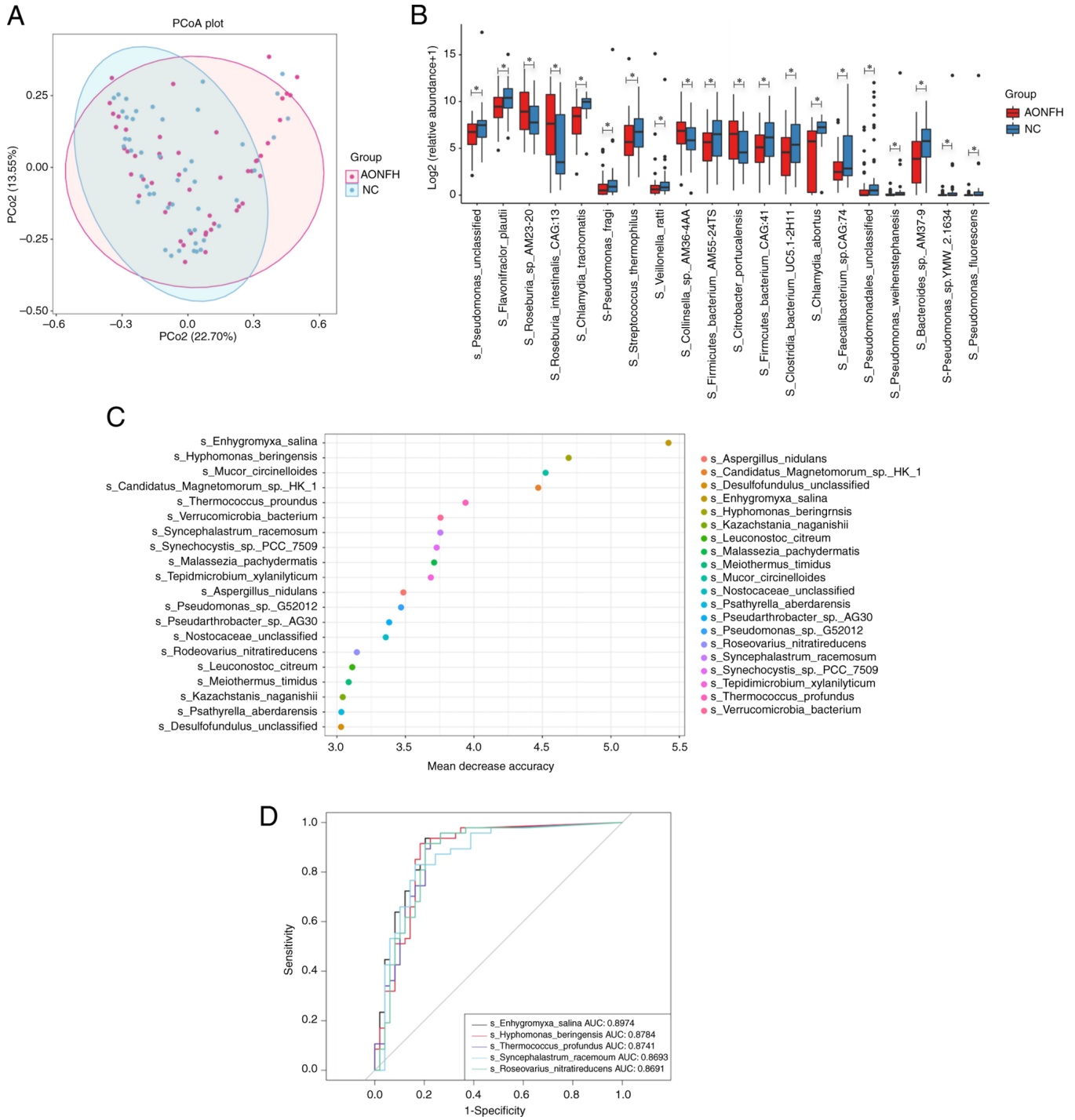

Figure 3. Differences in the gut microbiota in the AONFH and NC groups based on the metagenomic sequencing data. (A) PCoA analysis based on the Bray-Curtis distance matrix between the AONFH and NC groups at the species level (ANOSIM, R=0.02; P=0.06). (B) Relative abundance of the top 20 species enriched in the AONFH and NC groups. Data were presented as median ± interquartile range. (C) Performance of a random forest model classification as assessed using the R 'random forest' package. (D) Receiver operating characteristic curve displaying the top five biomarkers for distinguishing between the AONFH and NC groups. *P<0.05. AONFH, alcohol-induced osteonecrosis of the femoral head; NC, negative control; PCoA, principal coordinate analysis; ANOSIM, analysis of similarities; AUC, area under the curve.

Metabolite profiling and AONFH-related pathways. Pathway analysis demonstrated the detailed impact of AONFH-related alterations in metabolic networks (Fig. 5C). The most influential metabolic pathway had a pathway impact of >0.05 and $\log_{10}$(P-value)>0.3. A total of four metabolic pathways were identified as being disturbed in the fecal profiles of patients with AONFH, which included 'vitamin B6 metabolism', 'retinol metabolism', 'pentose and glucuronate interconversions' and 'glycerophospholipid metabolism'. KEGG enrichment analysis identified the most abundant metabolic pathways in the two groups (Fig. 6A). Based on P-values, pathway impact and enrichment ratios, the top two differentially expressed metabolic pathways were deemed to be 'vitamin B6 metabolism' and 'retinol metabolism'.

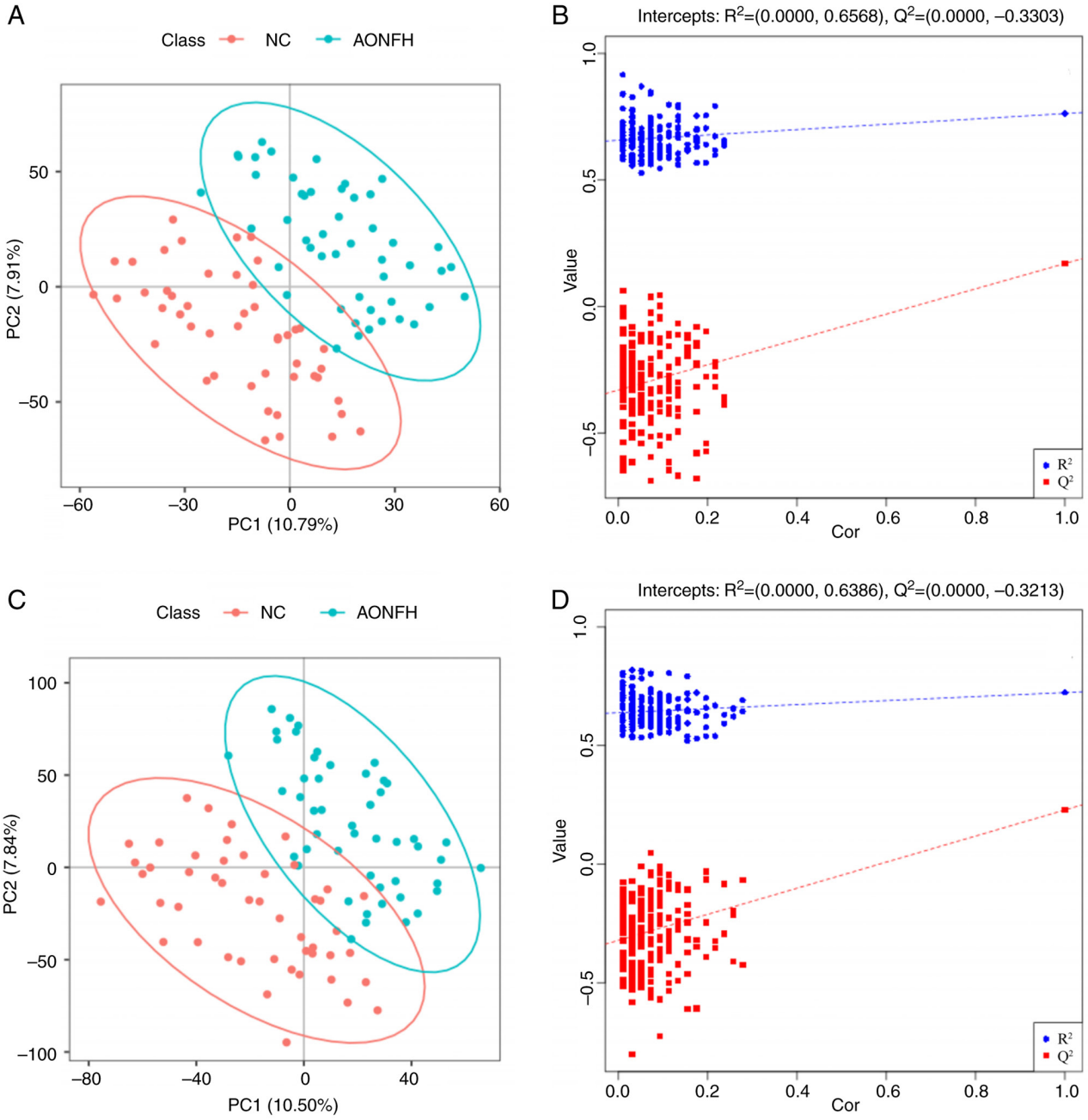

Figure 4. (A) Partial least squares discriminant analysis score plot in negative ion mode. (B) Permutation plot in negative ion mode. (C) Partial least squares discriminant analysis score plot in positive ion mode. (D) Permutation plot in positive ion mode. AONFH, alcohol-induced osteonecrosis of the femoral head; NC, negative control; PC, principal component; Cor, correlation coefficient.

A correlation matrix was next created using Spearman correlation and correlation network analyses to explore the potential relationships between changes in the GM and changes in metabolic product concentrations (Fig. 6B and Table SV). The levels of ptilosteroid b, 16-methyl-6z,9z,12z-heptadecatrienoic acid, allylestrenol, heptabarbital, n-benzoylaspartic acid, ezetimibe and vanilloylglycine were found to be positively correlated with the abundance of various genera, such as *Schizosaccharomyces*, *Oceanicella*, *Basidiobolus*, *Mortierella* and *Roseovarius*. The levels of kanzonol E, sophoracoumestan A, dicaffeoylputrescine, neobavaisoflavone, pentylbenzene, sophorapterocarpan A, pyrazine, ropivacaine, o-methylpongamol, erythrinin C and semilicoisoflavone B were negatively correlated with the abundance of various genera, such as *Phanerochaete*, *Ceratobasidium*, *Candidatus* Hodgkinia, *Smittium*, *Schizosaccharomyces* and *Syncephalis*.

Discussion

GM is an important symbiotic partner that facilitates the maintenance of physiology in animals and humans. In addition, it can regulate several aspects of host physiology, such as nutritional metabolism (5). The GM has also been reported to be implicated in a number of conditions, including neurodegenerative diseases (23), cancer (24), obesity (25) and Kashin-Beck disease (26). As the prime pathogenic factor contributing to AONFH, alcohol is largely metabolized within the gastrointestinal tract (27). Alcohol can alter GM composition,

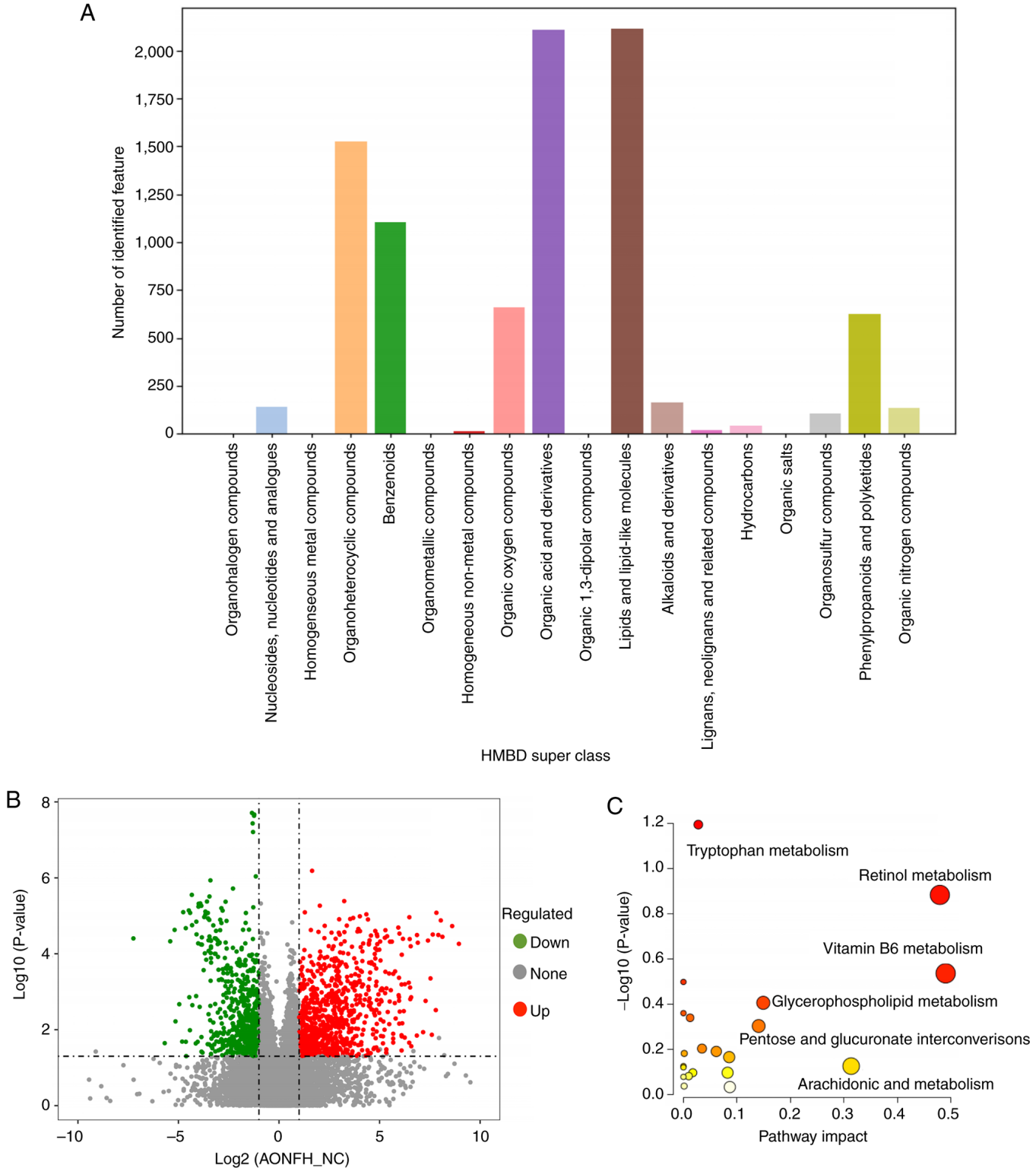

Figure 5. Fecal metabolomic changes and metabolic pathway in patients with AONFH. (A) The gut metabolites were identified by HMDB superclass analysis. (B) Volcano plot demonstrated the number of dysregulated metabolites in the feces of patients with AONFH compared with the NC group. (C) Computed metabolic pathways as a function of P-value and the pathway impacts of the key metabolites that were differentially expressed between the AONFH and NC groups. AONFH, alcohol-induced osteonecrosis of the femoral head; NC, negative control; HMDB, Human Metabolome Database.

impact the gut immune system and lead to downstream systemic effects on immune system communication with other organs (28). High levels of alcohol intake can result in nutrient malabsorption and deficiencies, including vitamin D, alter the gut microbiome and gut metabolites, affect the expression of bone metabolism-regulating hormones, induce osteoclast activation and influence GM composition (28). In addition, glucocorticoids can induce the loss of *Lactobacillus animalis* and its extracellular vesicles from the gut, which is associated with the pathogenesis of glucocorticoid-induced ONFH (29).

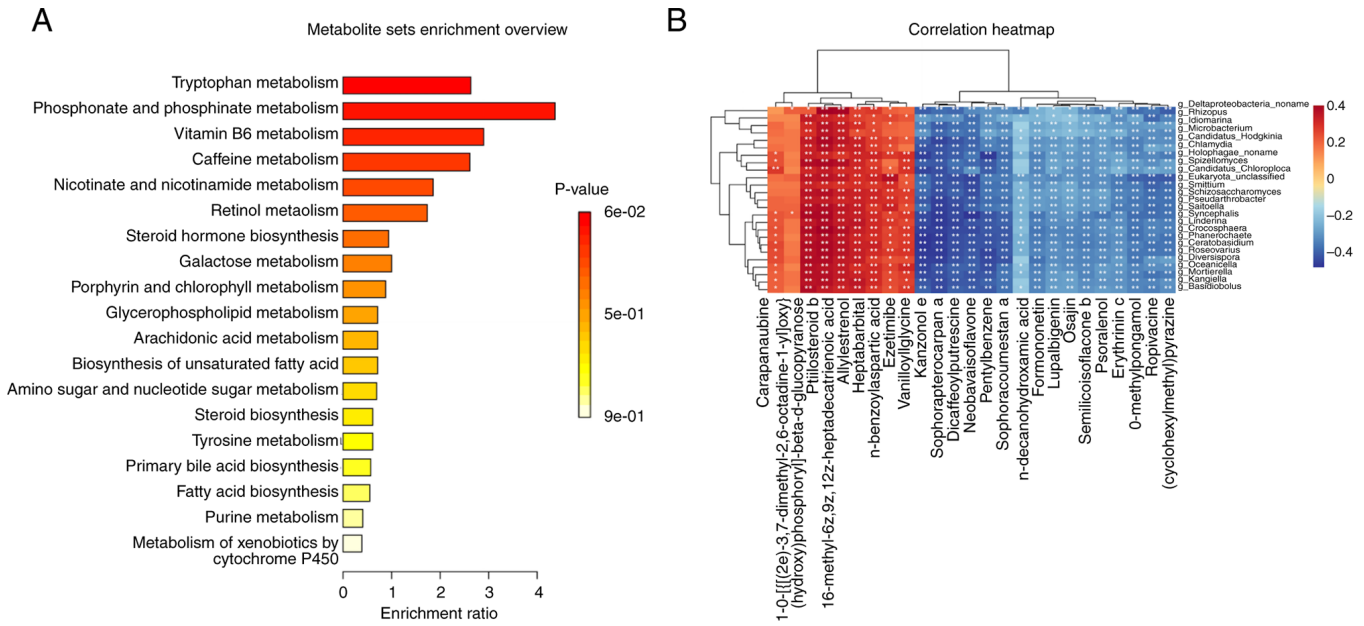

Figure 6. Differentially expressed metabolic pathways in patients with AONFH. (A) The most abundant metabolic pathways in the two groups as identified by Kyoto Encyclopedia of Genes and Genomes enrichment analysis. (B) Correlation between changes in the gut microbiota and the changes in metabolic product concentrations in patients with AONFH. AONFH, alcohol-induced osteonecrosis of the femoral head; NC, negative control.

Therefore, it is possible that the GM can serve a role in ONFH. However, to the best of our knowledge, no prior study has systematically investigated the role of GM and associated gut metabolites in the development of ONFH to date.

The results from the present study demonstrated that gut dysbiosis occurred in patients with AONFH, suggesting that alcohol may participate in AONFH pathogenesis by altering the GM composition. The 16S rDNA gene sequencing results demonstrated that *Pseudomonas*, Pseudomonadaceae, Oscillospiraceae, Firmicutes and *Streptococcus* were more abundant in the NC group compared with those in the AONFH group. By contrast, Burkholderiaceae, Buekholderiales, *Holdemanella*, Erysipelotrichaceae, *Klebsiella pneumoniae*, *Klebsiella*, Proteobacteria and Enterobacterales were more abundant in the AONFH group compared with those in the NC group. The metagenomics analysis results demonstrated that *Pseudomonas* was significantly less abundant in the AONFH group compared with those in the NC group.

In previous studies of clinical alcohol use disorder (AUD), the associated dysbiosis was characterized by a lower abundance of Bacteroidetes and *Akkermansia muciniphila* (30). In animal models of high-dose alcohol consumption, a decrease in bacterial diversity was observed, exemplified by fewer Bacteroidetes and Firmicutes (31,32), coupled with increased *Proteobacter*, Proteobacteria and *Actinobacter* (31-33). In particular, Proteobacteria is one of the most abundant phyla in the human GM and is frequently overrepresented in diseases, especially in those associated with an inflammatory phenotype, such as inflammatory bowel disease, asthma and chronic obstructive pulmonary disease (34). The present study demonstrated that Proteobacteria were more abundant in patients with AONFH, suggesting this species to be attributable to alcohol consumption. *Pseudomonas* is a member of the Proteobacteria phylum that has been reported to be associated with alcohol-related diseases and ONFH. This species is particularly prevalent in the intestine of rats with alcohol-related liver injury, where their abundance could be reduced by transplantation with fecal filtrate from a healthy rat (35). Liu *et al* (36) previously reported that *Pseudomonas aeruginosa* and *Pseudomonas putida* may be pathogens in patients with ONFH. However, the present study found decreased *Pseudomonas* abundance in patients with AONFH, suggesting that *Pseudomonas* abundance was decreased by alcohol consumption. The discrepancy between this study and Liu *et al* (36) may be due to all kinds of ONFH patients being included in their study, while only patients with AONFH were included in the present study. Another reason is that they reported the result at the species level, while the present study reported them at the genus level. *Klebsiella* and *Streptococcus* form another two members of the Proteobacteria phylum family. Individuals who consume excessive amounts of alcohol have previously been found to exhibit increased susceptibility to lung infection by *Streptococcus pneumoniae* and *Klebsiella pneumoniae* (37). Yuan *et al* (38) reported that ≤60% of individuals with non-alcoholic fatty liver disease in a Chinese cohort were infected with *Klebsiella pneumoniae*, a bacterial strain that produces alcohol as a byproduct of glucose. Taken together, these aforementioned studies suggest that alcohol consumption can increase susceptibility to *Klebsiella pneumoniae* infection and the subsequent excessive endogenous alcohol production due to GM alteration. Since *Klebsiella pneumoniae* and *Klebsiella* were found to be more abundant in the AONFH group in the present study, alcohol consumption may likely increase *Klebsiella pneumoniae* abundance in this group, resulting in the excessive production of endogenous alcohol and aggravation of AONFH pathogenesis.

Firmicutes and Bacteroidetes are two major phyla in the healthy human GM. They are documented to be involved in colonic metabolism through a complex metabolic energy-harvesting mechanism based on cross-feeding and co-metabolism (39). The Firmicutes/Bacteroidetes

ratio has been implicated in the predisposition to several disease states (40). Wang *et al* (26) previously reported that patients with Kashin-Beck disease were characterized by decreased Firmicutes levels and a significantly decreased Firmicutes/Bacteroidetes ratio. In addition, Firmicutes abundance was found to be positively associated with calcium absorption (41), which was significantly decreased in the presence of alcohol (42), a finding that was verified by Cheng *et al* (28). In the present study, it was demonstrated that Firmicutes levels were decreased in patients with AONFH, suggesting that alcohol consumption may contribute to AONFH pathogenesis by decreasing Firmicutes abundance.

ONFH develops because of varying degrees of necrosis in the local microenvironment (5). This can in turn lead to a number of pathological changes caused by erroneous metabolic processes, including intravascular fat embolism, endovascular coagulation, lipid metabolism, apoptosis and inhibition of angiogenesis (5). It can therefore be possible that alterations in certain metabolic molecular markers are evident in the bloodstream during the early stages of the ONFH pathological process. In the present study, several important gut microbial gene functions were identified, such as CDP-diacylglycerol biosynthesis I/II, L-histidine biosynthesis and the L-serine and glycine biosynthesis I superpathway. CDP-diacylglycerol is a critical intermediate in lipid metabolism, taking part in the synthesis of phosphatidylglycerol, cardiolipin and phosphatidylinositol (42). CDP-diacylglycerol synthase (CDS) produces CDP-diacylglycerol from phosphatidic acid and cytidine triphosphate (43). CDS has been reported to serve an important role in various processes, including mitochondrial function, signal transduction, membrane trafficking, secretion and cytoskeletal rearrangements (44). In the present study, CDP-diacylglycerol biosynthesis was identified as one of the most important gut microbial gene functions altered in patients with AONFH. Therefore, CDP-diacylglycerol and CDS may serve key roles in AONFH pathogenesis, but further studies are needed to investigate the underlying mechanism of this process.

A previous bioinformatics analysis performed by Yang *et al* (1) revealed that histidine, cysteine and methionine metabolism were associated with ONFH pathogenesis, where subsequent metabolic pathway analysis found that L-histidine is a key molecule in histidine metabolism and L-serine has a central role in cysteine and methionine metabolism. Histidine is an essential amino acid in mammals that can regulate gene expression, biological activity of proteins and signal transduction (45). By contrast, L-serine has been reported to promote osteoclast formation and therefore induce bone resorption (46). These aforementioned previous findings support the microbial gene function prediction results of the present study, suggesting that L-histidine and L-serine may serve regulatory roles in the pathology of AONFH.

In the present study, it was found that glycine biosynthesis may participate in the pathological process of ONFH. Betaine is a trimethyl derivative of glycine and an important nutrient for humans, which regulates a series of vital biological processes, including oxidative stress, inflammatory responses, osteoblast differentiation and apoptosis (47-49). Yang *et al* (50) previously reported that betaine is a potential pharmacotherapy option for alcohol-induced ONFH *in vivo*, since it was observed to exert a protective role against ethanol-induced suppression of osteogenesis and mineralization of human bone marrow mesenchymal stem cells.

Vitamin A is vital for a variety of bodily functions, including gene expression, reproduction, embryonic development and immune function (51). Whilst insufficient vitamin A intake can cause a number of adverse effects, including low bone density, excessive vitamin A consumption can also cause bone loss and increase the risk of fracture, leaving a narrow range of optimal dosage (52). As the biologically active form of vitamin A, retinol can enhance osteoblast proliferation and hinder osteoclast resorption (53). It has previously been reported that chronic alcohol consumption can mediate adverse effects on vitamin A metabolism, which can be directly associated with the development of alcohol-induced disease (54). In the present study, retinol metabolism was identified to be one of the most important AONFH-related pathways. Therefore, alcohol may disturb retinol metabolism in this disease, forming a part of AONFH pathogenesis. Vitamin B6 deficiency is common in individuals with alcoholism (55). This condition was previously found to be a potential risk factor for osteoporosis and bone fracture (56). Additionally, serum vitamin B6 concentration was observed to significantly associate inversely with the concentration of the bone resorption marker parathyroid hormone, whilst significantly associating positively with the concentration of 25-hydroxyvitamin D (57). Vitamin B6 deficiency may affect the mechanical property of the bone due to reduced cortical thickness, trabecular osteoid and coarse trabeculation (57). Therefore, alcohol may potentially induce vitamin B6 deficiency, which can disturb the balance between bone resorption and bone reconstruction in AONFH.

Dysfunction of lipid metabolism is reported to serve a crucial role in ONFH. A previous study reported different serum lipidomic profiles between patients with SONFH and healthy controls, where glycerophospholipids occupied a large part of this difference (58). In addition, it was reported that glycerophospholipids were distinguished in the bone trabecula and plasma of patients with ONFH compared with those in healthy controls, most glycerophospholipids were upregulated in patients with ONFH (59,60). Mei *et al* (61) previously reported that glycerophospholipid metabolism was the metabolic pathway that was the most significantly altered in rabbits with SONFH, suggesting it to be a potential pathway for the targeted intervention against SONFH. In the future, the detailed mechanism of how glycerophospholipid metabolism impacts AONFH requires further study.

In conclusion, the present study demonstrated that gut dysbiosis occurred in patients with AONFH, possibly causing alterations in gut metabolites. This altered GM profile and metabolites may serve as potential diagnostic markers for AONFH, even if the GM metabolites are from host cells or food in the intestinal tract. In particular, analysis of the interactions among alcohol, GM, metabolites and AONFH discussed in the present study may enhance the understanding of the mechanisms underlying AONFH pathogenesis. The findings from the present study regarding GM and metabolite changes may also facilitate the discovery of novel therapeutic targets. However, several research directions remain

that require further elucidation. Detection of additional biochemical indicators associated with bone metabolism is required to understand the relationship between the GM and biochemical indicators. This may in turn deepen the understanding into the role of GM in AONFH pathogenesis. In addition, since probiotics, prebiotics or symbiotics can regulate the GM (26), future studies are required to investigate the relationship among such substances, gut dysbiosis and AONFH.

Acknowledgements

Not applicable.

Funding

The present study was supported by the National Natural Science Foundation of China (grant no. 82074472), the Zhejiang Provincial Natural Science Foundation (grant no. LQ22H060003) and the Heluo Youth Talent Promotion Project (grant no. 2022HLTJ15).

Availability of data and materials

The data generated in the present study may be found in the China National Centre for Bioinformation repository for metagenomic sequencing (accession no. PRJCA021196; https://bigd.big.ac.cn/gsa/browse/CRA014109), for 16S rDNA analysis (accession no. PRJCA022064; https://bigd.big.ac.cn/gsa/browse/CRA014110) and metabolomics (accession no. PRJCA022518; https://ngdc.cncb.ac.cn/omix/release/OMIX005517).

Authors' contributions

CY, YL and BX contributed to the study conception and design. MM, YY and JG performed the experiments. Data collection and analysis were performed by CY, HL and YL. CY and BX confirm the authenticity of all the raw data. The manuscript was drafted by CY and BX and all authors commented on previous versions of the manuscript. All authors read and approved the final manuscript.

Ethics approval and consent to participate

The present study was approved by the ethics committee of Luoyang Orthopedic-Traumatological Hospital of Henan Province (approval no. KY2021-007-01) and the study was performed in accordance with The Declaration of Helsinki. All participants provided written informed consent for participation into the present study and the study protocols followed the ethical guidelines of The Declaration of Helsinki.

Patient consent for publication

Not applicable.

Competing interests

The authors declare that they have no competing interests.

References

1. Yang G, Zhao G, Zhang J, Gao S, Chen T, Ding S and Zhu Y: Global urinary metabolic profiling of the osteonecrosis of the femoral head based on UPLC-QTOF/MS. Metabolomics 15: 26, 2019.
2. Tan B, Li W, Zeng P, Guo H, Huang Z, Fu F, Gao H, Wang R and Chen W: Epidemiological study based on china osteonecrosis of the femoral head database. Orthop Surg 13: 153-160, 2021.
3. Yan Y, Wang J, Huang D, Lv J, Li H, An J, Cui X and Zhao H: Plasma lipidomics analysis reveals altered lipids signature in patients with osteonecrosis of the femoral head. Metabolomics 18: 14, 2022.
4. Seamon J, Keller T, Saleh J and Cui Q: The pathogenesis of nontraumatic osteonecrosis. Arthritis 2012: 601763, 2012.
5. Pouya F and Kerachian MA: Avascular necrosis of the femoral head: Are any genes involved? Arch Bone Jt Surg 3: 149-55, 2015.
6. Ticinesi A, Lauretani F, Milani C, Nouvenne A, Tana C, Del Rio D, Maggio M, Ventura M and Meschi T: Aging gut microbiota at the Cross-Road between nutrition, physical frailty, and sarcopenia: Is there a gut-muscle axis? Nutrients 9: 1303, 2017.
7. Lucas S, Omata Y, Hofmann J, Böttcher M, Iljazovic A, Sarter K, Albrecht O, Schulz O, Krishnacoumar B, Krönke G, *et al*: Short-chain fatty acids regulate systemic bone mass and protect from pathological bone loss. Nat Commun 9: 55, 2018.
8. Li JY, Chassaing B, Tyagi AM, Vaccaro C, Luo T, Adams J, Darby TM, Weitzmann MN, Mulle JG, Gewirtz AT, *et al*: Sex steroid deficiency-associated bone loss is microbiota dependent and prevented by probiotics. J Clin Invest 126: 2049-2063, 2016.
9. Wei X, Pushalkar S, Estilo C, Wong C, Farooki A, Fornier M, Bohle G, Huryn J, Li Y, Doty S and Saxena D: Molecular profiling of oral microbiota in jawbone samples of bisphosphonate-related osteonecrosis of the jaw. Oral Dis 18: 602-612, 2012.
10. Wang SC, Chen YC, Chen SJ, Lee CH and Cheng CM: Alcohol addiction, gut microbiota, and alcoholism treatment: A review. Int J Mol Sci 21: 6413, 2020.
11. Gabriel S, Ziaugra L and Tabbaa D: SNP genotyping using the Sequenom MassARRAY iPLEX platform. Curr Protoc Hum Genet: Chapter 2: Unit 2.12, 2009.
12. Logue JB, Stedmon CA, Kellerman AM, Nielsen NJ, Andersson AF, Laudon H, Lindström ES and Kritzberg ES: Experimental insights into the importance of aquatic bacterial community composition to the degradation of dissolved organic matter. ISME J 10: 533-545, 2015.
13. Callahan BJ, McMurdie PJ, Rosen MJ, Han AW, Johnson AJ and Holmes SP: DADA2: High-resolution sample inference from Illumina amplicon data. Nat Methods 13: 581-583, 2016.
14. Quast C, Pruesse E, Yilmaz P, Gerken J, Schweer T, Yarza P, Peplies J and Glöckner FO: The SILVA ribosomal RNA gene database project: Improved data processing and web-based tools. Nucleic Acids Res 41 (Database Issue): D590-D596, 2013.
15. Langmead B and Salzberg SL: Fast gapped-read alignment with Bowtie 2. Nat Methods 9: 357-359, 2012.
16. Peng Y, Leung HC, Yiu SM and Chin FY: IDBA-UD: A de novo assembler for single-cell and metagenomic sequencing data with highly uneven depth. Bioinformatics 28: 1420-1428, 2012.
17. Zhu W, Lomsadze A and Borodovsky M: Ab initio gene identification in metagenomic sequences. Nucleic Acids Res 38: e132, 2010.
18. Li W and Godzik A: Cd-hit: A fast program for clustering and comparing large sets of protein or nucleotide sequences. Bioinformatics 22: 1658-1659, 2006.
19. Buchfink B, Reuter K and Drost HG: Sensitive protein alignments at tree-of-life scale using DIAMOND. Nat Methods 18: 366-368, 2021.
20. Delinsky DC, Hill KT, White CA and Bartlett MG: Quantitation of the large polypeptide glucagon by protein precipitation and LC/MS. Biomed Chromatogr 18: 700-705, 2004.
21. Zheng JB, Xie YZ, Li F, Zhou Y, Qi LQ, Liu LB and Chen Z: Lactoferrin improves cognitive function and attenuates brain senescence in aged mice. J Functional Foods 65: 103736, 2019.
22. Long NP, Heo D, Kim HY, Kim TH, Shin JG, Lee A and Kim DH: Metabolomics-guided global pathway analysis reveals better insights into the metabolic alterations of breast cancer. J Pharm Biomed Anal 202:114134, 2021.
23. Zhang H, Chen Y, Wang Z, Xie G, Liu M, Yuan B, Chai H, Wang W and Cheng P: Implications of gut microbiota in neurodegenerative diseases. Front Immunol 13:785644, 2022.

24. Vivarelli S, Falzone L, Leonardi GC, Salmeri M and Libra M: Novel insights on gut microbiota manipulation and immune checkpoint inhibition in cancer (Review). Int J Oncol 59: 75, 2021.
25. Li R, Huang X, Liang X, Su M, Lai KP and Chen J: Integrated omics analysis reveals the alteration of gut microbe-metabolites in obese adults. Brief Bioinform 22: bbaa165, 2021.
26. Wang X, Ning Y, Li C, Gong Y, Huang R, Hu M, Poulet B, Xu K, Zhao G, Zhou R, *et al*: Alterations in the gut microbiota and metabolite profiles of patients with Kashin-Beck disease, an endemic osteoarthritis in China. Cell Death Dis 12: 1015, 2021.
27. Bishehsari F, Magno E, Swanson G, Desai V, Voigt RM, Forsyth CB and Keshavarzian A: Alcohol and Gut-Derived inflammation. Alcohol Res 38: 163-171, 2017.
28. Cheng M, Tan B, Wu X, Liao F, Wang F and Huang Z: Gut microbiota is involved in alcohol-induced osteoporosis in young and old rats through immune regulation. Front Cell Infect Microbiol 11: 636231, 2021.
29. Chen CY, Rao SS, Yue T, Tan YJ, Yin H, Chen LJ, Luo MJ, Wang Z, Wang YY, Hong CG, *et al*: Glucocorticoid-induced loss of beneficial gut bacterial extracellular vesicles is associated with the pathogenesis of osteonecrosis. Sci Adv 8: eabg8335, 2022.
30. Caslin B, Mohler K, Thiagarajan S and Melamed E: Alcohol as friend or foe in autoimmune diseases: A role for gut microbiome? Gut Microbes 13: 1916278, 2021.
31. Mutlu EA, Gillevet PM, Rangwala H, Sikaroodi M, Naqvi A, Engen PA, Kwasny M, Lau CK and Keshavarzian A: Colonic microbiome is altered in alcoholism. Am J Physiol Gastrointest Liver Physiol 302: G966-G978, 2012.
32. Dubinkina VB, Tyakht AV, Odintsova VY, Yarygin KS, Kovarsky BA, Pavlenko AV, Ischenko DS, Popenko AS, Alexeev DG, Taraskina AY, *et al*: Links of gut microbiota composition with alcohol dependence syndrome and alcoholic liver disease. Microbiome 5: 141, 2017.
33. Yan AW and Schnabl B: Bacterial translocation and changes in the intestinal microbiome associated with alcoholic liver disease. World J Hepatol 4: 110-118, 2012.
34. Rizzatti G, Lopetuso LR, Gibiino G, Binda C and Gasbarrini A: Proteobacteria: A common factor in human diseases. Biomed Res Int 2017: 9351507, 2017.
35. Yu L, Wang L, Yi H and Wu X: Beneficial effects of LRP6-CRISPR on prevention of alcohol-related liver injury surpassed fecal microbiota transplant in a rat model. Gut Microbes 11: 1015-1029, 2020.
36. Liu C, Li W, Zhang C, Pang F and Wang DW: Previously unexplored etiology for femoral head necrosis: Metagenomics detects no pathogens in necrotic femoral head tissue. World J Clin Cases 10: 2138-2146, 2022.
37. Raju SV, Painter RG, Bagby GJ, Nelson S and Wang G: Response of differentiated human airway epithelia to alcohol exposure and klebsiella pneumoniae challenge. Med Sci (Basel) 1: 2-19, 2013.
38. Yuan J, Chen C, Cui J, Lu J, Yan C, Wei X, Zhao X, Li N, Li S, Xue G, *et al*: Fatty liver disease caused by high-alcohol-producing klebsiella pneumoniae. Cell Metab 30: 675-688.e7, 2019.
39. Cheng L, Chen Y, Zhang X, Zheng X, Cao J, Wu Z, Qin W and Cheng K: A metagenomic analysis of the modulatory effect of Cyclocarya paliurus flavonoids on the intestinal microbiome in a high-fat diet-induced obesity mouse model. J Sci Food Agric 99: 3967-3975, 2019.
40. Jandhyala SM, Talukdar R, Subramanyam C, Vuyyuru H, Sasikala M and Nageshwar Reddy D: Role of the normal gut microbiota. World J Gastroenterol 21: 8787-8803, 2015.
41. Whisner CM, Martin BR, Nakatsu CH, Story JA, MacDonald-Clarke CJ, McCabe LD, McCabe GP and Weaver CM: Soluble corn fiber increases calcium absorption associated with shifts in the gut microbiome: A randomized Dose-Response trial in Free-Living pubertal females. J Nutr 146: 1298-1306, 2016.
42. Qamar N, Castano D, Patt C, Chu T, Cottrell J and Chang SL: Meta-analysis of alcohol induced gut dysbiosis and the resulting behavioral impact. Behav Brain Res 376: 112196, 2019.
43. Jennings W and Epand RM: CDP-diacylglycerol, a critical intermediate in lipid metabolism. Chem Phys Lipids 230: 104914, 2020.
44. Wang X, Devaiah SP, Zhang W and Welti R: Signaling functions of phosphatidic acid. Prog Lipid Res 45: 250-278, 2006.
45. Klumpp S and Krieglstein J: Phosphorylation and dephosphorylation of histidine residues in proteins. Eur J Biochem 269: 1067-1071, 2002.
46. Ogawa T, Ishida-Kitagawa N, Tanaka A, Matsumoto T, Hirouchi T, Akimaru M, Tanihara M, Yogo K and Takeya T: A novel role of L-serine (L-Ser) for the expression of nuclear factor of activated T cells (NFAT)2 in receptor activator of nuclear factor kappa B ligand (RANKL)-induced osteoclastogenesis in vitro. J Bone Miner Metab 24: 373-379, 2006.
47. Veskovic M, Mladenovic D, Milenkovic M, Tosic J, Borozan S, Gopcevic K, Labudovic-Borovic M, Dragutinovic V, Vucevic D, Jorgacevic B, *et al*: Betaine modulates oxidative stress, inflammation, apoptosis, autophagy, and Akt/mTOR signaling in methionine-choline deficiency-induced fatty liver disease. Eur J Pharmacol 848: 39-48, 2019.
48. Shi H, Wang XL, Quan HF, Yan L, Pei XY, Wang R and Peng XD: Effects of betaine on LPS-Stimulated activation of microglial M1/M2 phenotypes by suppressing TLR4/NF-κB pathways in N9 cells. Molecules 24: 367, 2019.
49. Li C, Wang Y, Li L, Han Z, Mao S and Wang G: Betaine protects against heat exposure-induced oxidative stress and apoptosis in bovine mammary epithelial cells via regulation of ROS production. Cell Stress Chaperones 24: 453-460, 2019.
50. Yang Q, Yin W, Chen Y, Zhu D, Yin J, Zhang C and Gao Y: Betaine alleviates alcohol-induced osteonecrosis of the femoral head via mTOR signaling pathway regulation. Biomed Pharmacother 120: 109486, 2019.
51. Conaway HH, Henning P and Lerner UH: Vitamin a metabolism, action, and role in skeletal homeostasis. Endocr Rev 34: 766-797, 2013.
52. Yee MMF, Chin KY, Ima-Nirwana S and Wong SK: Vitamin A and Bone Health: A review on current evidence. Molecules 26: 1757, 2021.
53. Vu AA, Kushram P and Bose S: Effects of Vitamin A (Retinol) release from calcium phosphate matrices and Porous 3D printed scaffolds on bone cell proliferation and maturation. ACS Appl Bio Mater 5: 1120-1129, 2022.
54. Clugston RD and Blaner WS: The adverse effects of alcohol on vitamin A metabolism. Nutrients 4: 356-371, 2012.
55. Tobias SL, van der Westhuyzen J, Davis RE, Icke GC and Atkinson PM: Alcohol intakes and deficiencies in thiamine and vitamin B6 in black patients with cardiac failure. S Afr Med J 76: 299-302, 1989.
56. Wang J, Chen L, Zhang Y, Li CG, Zhang H, Wang Q, Qi X, Qiao L, Da WW, Cui XJ, *et al*: Association between serum vitamin B6 concentration and risk of osteoporosis in the middle-aged and older people in China: A cross-sectional study. BMJ Open 9: e028129, 2019.
57. Masse PG, Pritzker KP, Mendes MG, Boskey AL and Weiser H: Vitamin B6 deficiency experimentally-induced bone and joint disorder: Microscopic, radiographic and biochemical evidence. Br J Nutr 71: 919-932, 1994.
58. Wang XY, Zhang LL, Jiang C, Hua BX, Ji ZF, Fan WS, Gong LJ, Zhu L, Wang XD and Yan ZQ: Altered lipidomic profiles in patients with and without osteonecrosis of the femoral head after 1-month glucocorticoid treatment. Clin Transl Med 11: e298, 2021.
59. Zhu W, Chen T, Ding S, Gang Y, Xu Z, Xu K, Zhang S, Ma T and Zhang J: Metabolomic study of the bone trabecula of osteonecrosis femoral head patients based on UPLC-MS/MS. Metabolomics 12: 48, 2016.
60. Liu X, Li Q, Sheng J, Hu B, Zhu Z, Zhou S, Yin J, Gong Q, Wang Y and Zhang C: Unique plasma metabolomic signature of osteonecrosis of the femoral head. J Orthop Res 34: 1158-1167, 2016.
61. Mei R, Chen D, Zhong D, Li G, Lin S, Zhang G, Chen K and Yu X: Metabolic profiling analysis of the effect and mechanism of gushiling capsule in rabbits with Glucocorticoid-Induced osteonecrosis of the femoral head. Front Pharmacol 13: 845856, 2022.